An Edge-Minimization Problem for Regular Polygons

Ralph H. Buchholz <teufel_pi@yahoo.com>
Warwick de Launey <warwickdelauney@earthlink.net>

Submitted: Aug 19, 2008; Accepted: Jul 11, 2009; Published: Jul 24, 2009
Mathematics Subject Classification: 05B45, 52C20

Abstract

In this paper we will examine the following problem: What is the minimum number of unit edges required to construct k identical size regular polygons in the plane if sharing of edges is allowed?

1 Introduction

In this paper we will examine the following problem:

Question 1 *What is the minimum number of sides required to construct k identical size regular polygons in the plane if sharing of sides is allowed?*

Below is an optimal configuration of 10 heptagons which reuses 11 sides. There will

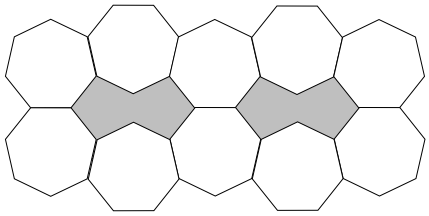

Figure 1: Optimal configuration for 10 heptagons

usually be more than one configuration of k polygons which minimizes the number of sides (see Figure 2) so we pose the following harder problem.

Question 2 *What are all the optimal configurations?*

This second question is particularly interesting because these optimal configurations are likely to arise in nature. For example, there are the quasi-periodic Penrose tilings which

have been found to correspond to the arrangement of atoms in certain types of non-stick surfaces; biological cell growth on a surface around fixed obstacles; growth of soap films between parallel walls [6]; large-scale convection cells on the surface of the sun and other stars—even the hexagonal structure at the pole of Saturn may be a portion of an energy minimisation tiling of the surface of that planet.

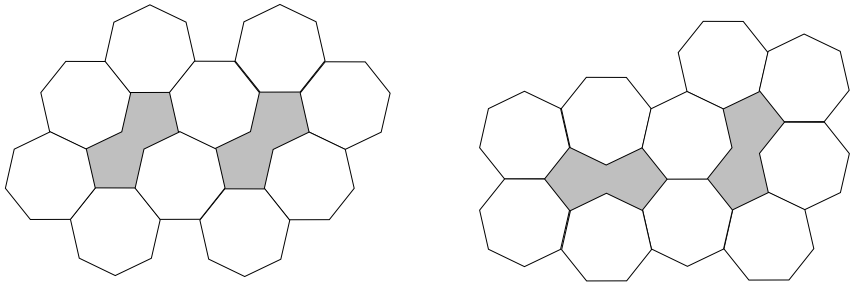

Figure 2: The two other optimal configurations for 10 heptagons

The earliest reference to Question 1 appears to be an article of Harary and Harborth ([5]) where they provide a complete answer for the square, the equilateral triangle, and the regular hexagon. They introduce a spiral algorithm which (for each of the three shapes) allows them to build up a sequence of optimal configurations $C_1, C_2, \ldots, C_k, \ldots$, such that C_{k+1} is obtained from C_k by adding a single cell.

The authors of the present paper have been studying this problem since the early 1980s (see [1]) and related papers have recently begun to appear. For example, a series of papers ([12], [13], [14], [16]) describe the impact of minimum perimeter tilings on the design of databases and they obliquely make reference to the square spiral algorithm. More explicitly, the spiral algorithm applied to squares can be found in [9] and there is the suggestion of the same process applied to squares, triangles and hexagons in Sloane's Online Integer Sequence Encyclopedia [10], (see A137228, A078633, A135708)—the last one is derived from the work in [8]. While the seminal tome on tilings in the literature ([3]) does not contain a direct reference to this problem, it does contain many of the tilings we consider in this paper. Finally, interesting animations of pentagonal near-tilings are provided on the Wolfram site (see [7] and [11]).

It happens that the square, the equilateral triangle and the hexagon are the only regular polygons which tessellate the plane. The existence of these tessellations seems to be the key to Harary and Harborth's success for $n = 3, 4$ and 6. When the n-gon does not tessellate the plane, there are some internal unshared sides. This leads to complications which seem to make the questions for general n much harder. In this paper, we obtain asymptotically optimal configurations for all n. Our approach is to construct *near-tessellations* and then apply a spiral allgorithm. These near tessellations are formed by putting together minimal cycles of ngons. This is possible because the minimal cycles always have length $3, 4$ or 6. For some n, there are uncountably many near-tessellations each producing asymptotically optimal configurations. To prove the resulting configura-

tions are in fact asymptotically optimal, we use a correspondence between configurations and planar graphs.

2 Configurations in General

2.1 Orientation of the Polygons

Let n be odd. Whenever the bottom side of an n-gon is horizontal, the uppermost extremity of the n-gon consists of a vertex lying directly above the center of the bottom side. In this case, we say the n-gon is oriented upwards. Similarly, we say the n-gon is oriented downwards if the vertex lies at the bottom of the n-gon and the horizontal side lies at the top. In both cases, we say the n-gons are properly oriented. When n is even, an n-gon is properly oriented if the top and bottom sides are both horizontal. Figure 3 illustrates examples of each of these oriented polygons. Notice that, after an appropriate

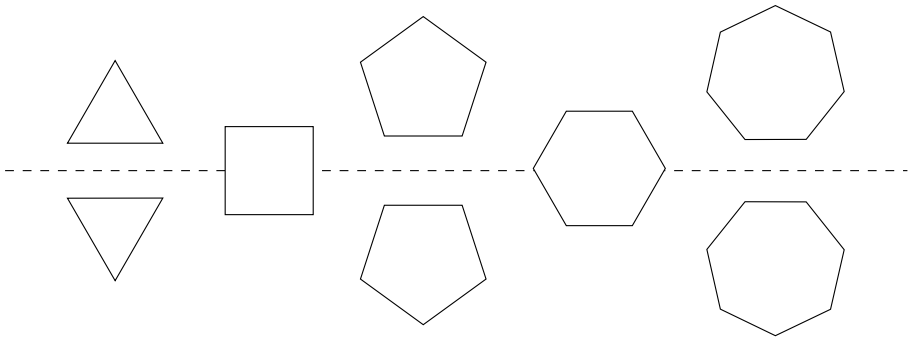

Figure 3: Properly oriented polygons with 3-7 sides

rotation, all configurations contain at least one properly oriented n-gon. When n is even, it is clear by symmetry that any n-gon sharing a side with a properly oriented polygon is also properly oriented. Figure 4 shows two superimposed properly oriented n-gons of opposite orientations. The symmetry of the figure indicates that the side A of the solid

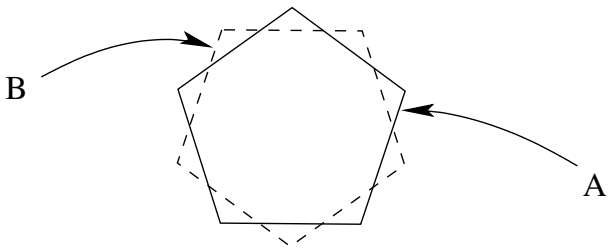

Figure 4: Superimposed properly oriented polygons

n-gon is parallel to the side B of the dashed n-gon, and that no other side of the dashed

n-gon is parallel to the side A. Thus, no matter how one manœuvres the dashed n-gon, if it shares the side A, then it will be properly oriented with orientation opposite to that of the solid n-gon.

Proposition 1 *Suppose a configuration contains a single properly oriented n-gon. Then all n-gons in the configuration are properly oriented. Moreover, for odd n, adjacent polygons have opposite orientation.*

2.2 Polygonal Configurations and Circle Configurations

Given a connected configuration of side-sharing polygons, one can form, by drawing inside each polygon a maximal inscribed circle, a connected configuration of touching circles. Figure 5 illustrates the construction. Notice that reduction to a circle configuration loses

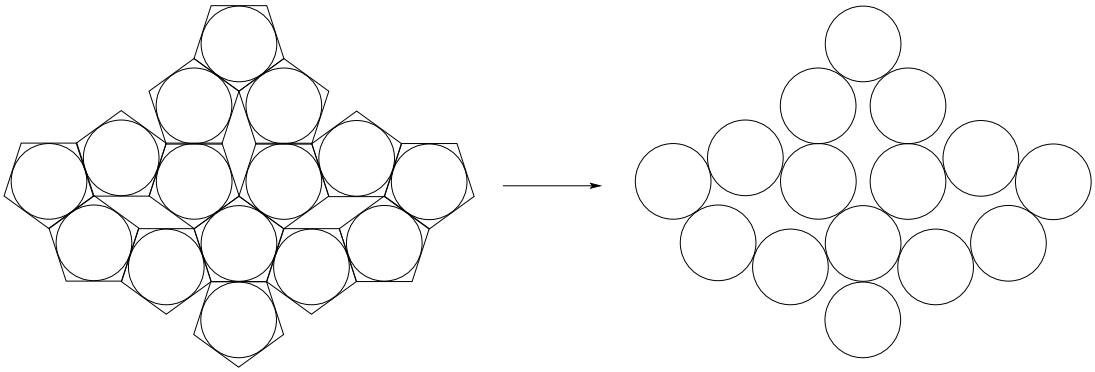

Figure 5: Reduction to a circle configuration

the orientation information. Nevertheless, circle configurations capture important features of the full problem. In particular,

Proposition 2 *In a circle configuration corresponding to a polygon configuration, two circles touch iff their corresponding polygons share an edge.*

In general, a circle configuration is an arrangement of identically-sized circles in the plane so that circles may touch but not overlap. A circle configuration is connected if there is a way to move between any pair of circles by passing along a sequence of touching circles.

Most circle configurations cannot be obtained by reduction from a polygon configuration. However, the following question regarding general circle configurations is particularly relevant to our investigation of polygonal configurations.

Question 3 *What is the maximum number of pairs of touching circles possible in a configuration of v circles?*

2.3 Configurations and Planar Graphs

Each configuration of n-gons in the plane yields a planar graph G where

- each node corresponds to an n-gon in the configuration, and
- two nodes are joined if they correspond to side-adjacent n-gons.

Let v denote the number of nodes, f denote the number of faces, and e denote the number of edges. By Euler's formula,

$$f = e - v + 2\,. \tag{1}$$

In general, there are several internal faces and one external face. Each internal face is bounded by a closed walk, the boundary of the face. Think of the closed walk as oriented clockwise. The boundary of the external face is oriented counterclockwise. If all of the boundaries of all of the faces are traversed, each edge in the graph is traversed twice, once in each direction. Thus if the i-th face has a boundary walk of length c_i, then

$$2e = c_1 + c_2 + \cdots + c_f\,. \tag{2}$$

If a boundary contains a node of degree 1, then the closed walk enclosing the face will traverse some edges in the boundary twice—once in each direction.

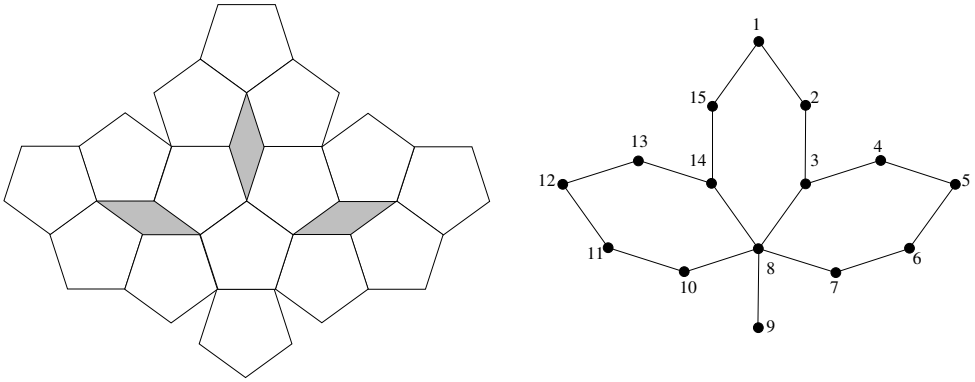

Figure 6: A configuration of pentagons and its corresponding planar graph

Example 1 *In Figure 6 we show a configuration of 15 pentagons and the corresponding planar graph G with labeled nodes. G contains $v = 15$ nodes, $e = 17$ edges and $f = 4$ faces. The boundary walks for the three internal cycles are $(1, 2, 3, 8, 14, 15)$, $(3, 4, 5, 6, 7, 8)$, and $(8, 10, 11, 12, 13, 14)$. The boundary walk for the external cycle is $(1, 2, 3, 4, 5, 6, 7, 8, 9, 8, 10, 11, 12, 13, 14, 15)$. Notice that the edge $(8, 9)$ is traversed twice - once in each direction.*

Proposition 3 *Let n denote the number of sides of a polygon. When n is odd, the corresponding planar graph is bipartite. In particular, all cycles have even length.*

2.4 Asymptotics

An asymptotic answer to Question 1 is now possible. By (1), maximizing the number of shared sides e in a configuration of v n-gons is equivalent to maximizing the number of faces f. Equation (1) also implies

$$\frac{e}{f-1} = 1 + \frac{v-1}{f-1}\,.$$

Therefore, maximizing f for fixed v is equivalent to minimizing $e/(f-1)$. In the next subsection we will show that for each n there is a minimum length $c_{\min} \in \{3, 4, 6\}$ for the boundary of any face. Under the assumption that $c_{\min}$ is well defined for each n, (2) then implies

$$\frac{e}{f-1} \geq \frac{1}{2}\left(c_{\min} + \frac{c_1}{f-1}\right)\,,$$

where c_1 is the length of the external cycle. In order to exhibit configurations which are at least asymptotically optimal, it is therefore sufficient to find configurations whose internal faces all have size $c_{\min}$, and whose external faces have size dominated by f.

2.5 Small Cycles of Circles

We use the term *necklace* to denote a finite collection of non-overlapping congruent circles for which every circle touches precisely two others. Before determining the value of $c_{\min}$, we consider small necklaces of circles. It happens that only cycles of length 3, 4 and 6 need be considered (see Figure 7 for examples). The 3 cycle is unique. On the other

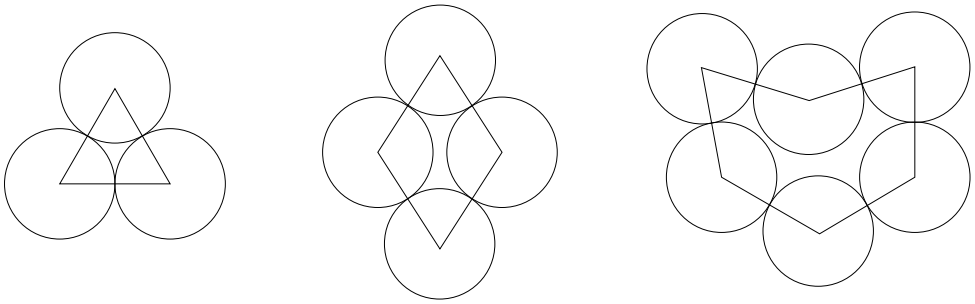

Figure 7: 3, 4, and 6 cycles

hand, there are many possible 4 cycles, all of them symmetric in the sense that the quadrilateral subtended by the centers of the circles have alternating internal angles equal. The situation for 6 cycles is markedly different, greatly complicating the situation for n-gons with n odd. Note that the internal angles can all be different, and that one of the angles can even be greater than π—thus creating a concave cycle.

2.6 Minimal Polygon Necklaces

We extend the notion of a necklace to include regular polygons, but two polygons are allowed to touch only if they share an entire edge. The immediate goal is to determine how the smallest number $c_{\min}$ of polygons in an n-gon necklace depends on the number n. Figure 8 shows the three non-isomorphic minimal necklaces for $n = 11$.

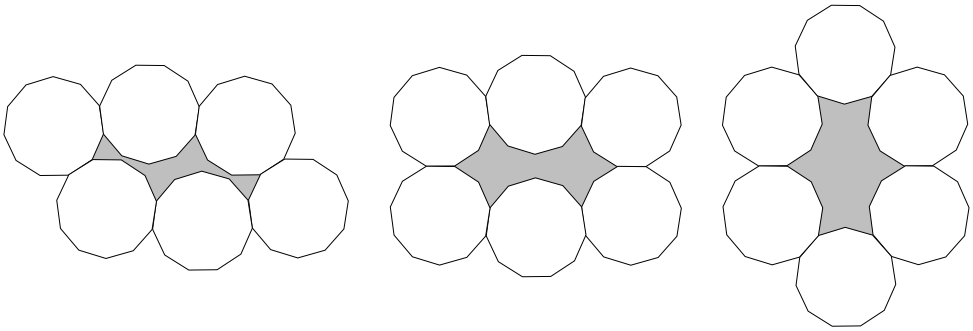

Figure 8: The minimal 11-gon necklaces

Consider a face with boundary equal to the closed walk $v_1, v_2, \ldots, v_c, v_{c+1} = v_1$. Let $-\pi \leq \alpha_i < \pi$ denote the angle turned to the right as we pass the node v_i. Then, because we wind around the interior of the face exactly once as we traverse the closed walk,

$$2\pi = \alpha_1 + \alpha_2 + \cdots + \alpha_c \,. \tag{3}$$

The angle α_i is called the *change in bearing* as we pass through vertex v_i.

Consider what happens in the corresponding polygon configuration as we move around a boundary. Each vertex in the planar graph is associated with a polygon in the corresponding configuration, therefore each cycle in the planar graph corresponds to a necklace of polygons. If the necklace contains c polygons, then the necklace contains cn sides, of which c are shared. If there are I edges on the interior border, the remaining $E = cn - I - 2c$ are on the outside of the necklace. Let E_i and I_i respectively denote the number of external and internal polygon sides contributed to the necklace by the the i-th polygon. Then

$$cn = 2c + \sum_{i=1}^{c} E_i + \sum_{i=1}^{c} I_i \,. \tag{4}$$

Figure 9 shows that $\alpha_i = (E_i - I_i)\frac{\pi}{n}$. Thus

$$2n = \sum_{i=1}^{c} (E_i - I_i) \,. \tag{5}$$

Consequently,

$$\frac{n(c-2)}{2} = c + \sum_{i=1}^{c} I_i \,. \tag{6}$$

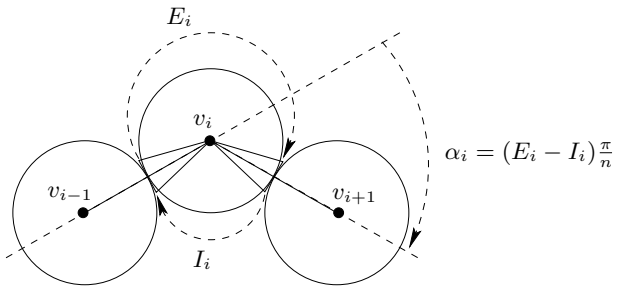

Figure 9: Change in bearing versus the number of internal and external sides

We can now use this fundamental equation to determine $c_{\min}$ for all possible n-gons. The smallest possible cycle occurs when $c = 3$. As $I_1 = I_2 = I_3 = I$, equation (6) becomes

$$n = 6(1 + I).$$

So if $n \equiv 0 \pmod 6$, then $(I_1, I_2, I_3) = \left(\frac{n}{6} - 1, \frac{n}{6} - 1, \frac{n}{6} - 1\right)$ is a solution—for which the hexagon is the smallest example.

The next-smallest necklaces are 4-cycles. Symmetry forces $I_1 = I_3$ and $I_2 = I_4$, so (6) becomes

$$n = 4 + 2I_1 + 2I_2. \tag{7}$$

Clearly, n must be even, so let $n = 2m$ and consider the cases of even and odd m. If $m = 2k$ then (7) becomes $2k-2 = I_1+I_2$, which has a particular solution of $(I_1, I_2) = (k-1, k-1)$—the smallest example being a square. If $m = 2k + 1$, then (7) becomes $2k - 1 = I_1 + I_2$, which has a particular solution of $(I_1, I_2) = (k - 1, k)$—with the decagon as the smallest example. All even n-gons now have either a minimal cycle of length three or length four.

For odd n we show that odd length cycles are impossible and we also eliminate 4-cycles. Let $n = 2m + 1$ and $c = 2k + 1$, so (6) becomes

$$(2m + 1)(2k - 1) = 2\left(2k + 1 + \sum_{i=1}^{2k+1} I_i\right),$$

which is impossible to solve over the integers (the left side is odd, and the right side is even). In particular, no 3-cycles or 5-cycles can occur. Next, if 4-cycles are possible then, as above, symmetry would force $I_1 = I_3$, $I_2 = I_4$, which means

$$2m + 1 = 4 + 2I_1 + 2I_2$$

from equation 7. This is also impossible.

Now we simply need to demonstrate the existence of solutions for a 6-cycle. Equation (6) becomes

$$2n = I_1 + I_2 + I_3 + I_4 + I_5 + I_6 + 6.$$

We attempt to solve a two parameter specialization by setting $(I_1, I_2, I_3, I_4, I_5, I_6) = (a, a, b, a, a, b)$ and $n = 2m + 1$, namely,

$$2m = 2a + b + 2.$$

Since we require that the 6-cycle not self-intersect, we have the inequalities

$$\frac{\pi}{3} \leq (a+1)\frac{2\pi}{n} \leq \pi \quad \text{and} \quad \frac{\pi}{3} \leq (b+1)\frac{2\pi}{n} \leq \pi.$$

For $m = 3k$, $3k+1$, $3k+2$, particular solutions to $2m = 2a + b + 2$ and the inequalities are $(a, b) = (2k-1, 2k)$, $(2k, 2k)$ and $(2k+1, 2k)$, respectively.

All this proves the following:

Proposition 4 *The smallest edge-sharing necklace for an n-gon is a*

$$\begin{cases} 3\text{-}cycle & for\ n \equiv 0 \pmod 6 \\ 4\text{-}cycle & for\ n \equiv 2, 4 \pmod 6 \\ 6\text{-}cycle & for\ n \equiv 1, 3, 5 \pmod 6. \end{cases}$$

2.7 Classification of 4-cycle necklaces

Notice that 4-cycle necklaces occur when $n \equiv \pm 2 \pmod 6$. The symmetry imposed by the 4 incircles forces these necklaces to always have at least the cyclic group C_2 as a symmetry group. However, whenever n is a multiple of four, then C_4 is possible as well. If $\alpha_1, \ldots, \alpha_4$ denote the four bearings of the 4-cycle, then symmetry forces $\alpha_1 = \alpha_3$, $\alpha_2 = \alpha_4$ and $\alpha_1 = \pi - \alpha_2$. Translating this into the internal edge counts leads to

$$(I_1, I_2, I_3, I_4) = \left(m, \frac{n}{2} - m - 2, m, \frac{n}{2} - m - 2\right),$$

where m is constrained by the non-overlapping requirement $\frac{\pi}{3} < (m+1)\frac{2\pi}{n}$. Notice that the sum of the internal edges is fixed for each polygon. All such m are possible, and to avoid double counting, $(m+1)\frac{2\pi}{n} \leq \frac{\pi}{2}$ is required, which leads to

$$\frac{n}{6} - 1 < m \leq \frac{n}{4} - 1.$$

Examples of 4-cycles for small n are shown in Table 1. The number of 4-cycle necklaces, $N_4(n)$, is now easy to obtain:

$$N_4(n) = \left\lfloor \frac{n}{4} - 1 \right\rfloor - \left\lceil \frac{n}{6} - 1 \right\rceil \quad \text{for } n \equiv \pm 2 \pmod 6.$$

n	I_1	I_2	I_3	I_4	symmetry
4	0	0	0	0	C_4
8	1	1	1	1	C_4
10	1	2	1	2	C_2
14	2	3	2	3	C_2
16	2	4	2	4	C_2
	3	3	3	3	C_4
20	3	5	3	5	C_2
	4	4	4	4	C_4
22	3	6	3	6	C_2
	4	5	4	5	C_2
26	4	7	4	7	C_2
	5	6	5	6	C_2

Table 1: 4-cycle necklaces

2.8 Computational search for 6-cycle necklaces

With 6-cycle polygonal necklaces, unlike the 4-cycle case, nothing can be inferred about the symmetry of the discrete case from the continuous case. In particular, the possible 6 internal arc-lengths of a 6-circle necklace can all be distinct. However, a systematic taxonomy of 6-polygon necklaces for small polygons does not reveal any corresponding asymmetric (or concave) necklaces—all examples to date are convex and have either 2, 3, or 6-fold symmetry.

For a regular n-gon we denote the incircle radius by r_n, the circumcircle radius by R_n, and the angle subtended at the centre by a side by $\theta_n = 2\pi/n$. The search begins by fixing two n-gons with their centres on the x-axis at $P_1 = (r_n, 0)$ and $P_2 = (-r_n, 0)$ (see Figure 10). The next three n-gons are centred at P_3, P_4 and P_5, sharing an edge with their

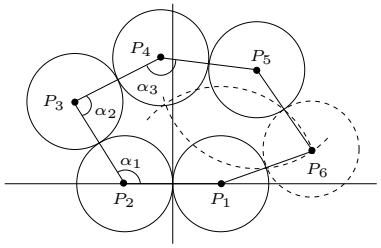

Figure 10: Setup for the computational search

respective neighbours. The discrete positions allowed for these three n-gons are defined by specifying three bearings $\alpha_i = m_i\theta_n$ where the m_i are arbitrary integer parameters ranging from 1 to $n-1$. By intersecting two circles of radius $2r_n$, centred at P_5 and P_1, possible positions of the last n-gon, at P_6 can be determined. The vectors $\overline{P_5P_6}$ and $\overline{P_6P_1}$ are only allowed to come from a discrete set, namely the $2n$-th roots of unity (see section 2.9). All

distances between pairs of non-adjacent points in $\{P_1, P_2, P_3, P_4, P_5, P_6\}$ are computed—a configuration fails if any such distance is less than $2r_n$ (due to overlap) and passes if all such distances are greater than $2R_n$. Any remaining "undecided" configurations can be subjected to a check using the roots of unity representation, described in section 2.9.

If the number of interior (non-shared) edges on each n-gon are respectively denoted by $(I_1, I_2, I_3, I_4, I_5, I_6)$, as one traverses the inside of the 6-cycle starting at P_2 say, then

$$I_i = \frac{\alpha_i}{\theta_n} - 1.$$

Table 2 shows the results for odd n-gons with up to 13 sides. In particular, extending this table up to 301 sides reveals that odd n-gons with $n \equiv 0 \pmod 3$ have 6-cycles with 2, 3 or 6-fold symmetry—i.e., 6-cycles of the form (a, b, c, a, b, c), (a, b, a, b, a, b), or (a, a, a, a, a, a). When $n \equiv \pm 1 \pmod 6$ the 6-cycles only have 2-fold symmetry—i.e., an

n	I_1	I_2	I_3	I_4	I_5	I_6	symmetry
3	0	0	0	0	0	0	C_6
5	0	1	1	0	1	1	C_2
7	1	2	1	1	2	1	C_2
9	1	3	2	1	3	2	C_2
	1	3	1	3	1	3	C_3
	2	2	2	2	2	2	C_6
11	1	4	3	1	4	3	C_2
	2	4	2	2	4	2	C_2
	2	3	3	2	3	3	C_2
13	2	5	3	2	5	3	C_2
	2	4	4	2	4	4	C_2
	3	4	3	3	4	3	C_2

Table 2: Six-cycle necklaces

interior of (a, b, c, a, b, c).

The total number of distinct necklaces, $N_6(n)$, for each n is very regular (see Figure 11) and is predicted by the following formula (proven later).

Theorem 2.1

$$N_6(n) = \begin{cases} \lfloor (i+1)^2/2 \rfloor - 1 & \text{if } n \equiv 3 \pmod 6 \\ \lfloor (i+1)^2/2 \rfloor - \lfloor (i+1)/2 \rfloor & \text{if } n \equiv \pm 1 \pmod 6, \end{cases}$$

where $i := \lfloor (n+3)/6 \rfloor$.

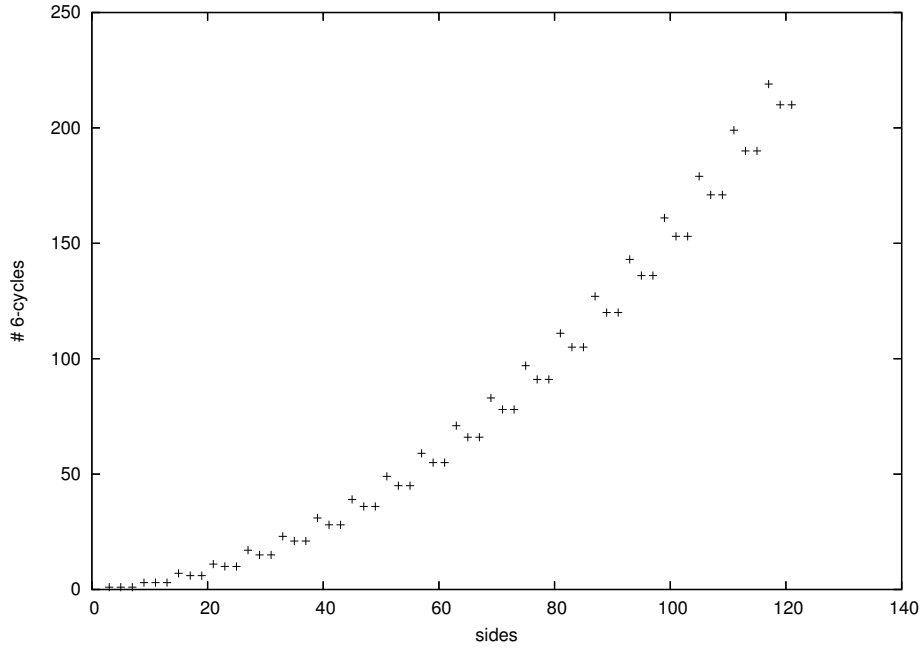

Figure 11: The number of 6-cycle necklaces

2.9 Roots-of-unity representation

An instructive way to represent these cycles and near-tilings is with the aid of roots of unity. For even n, the distance between the centres of any two side-sharing n-gons can be represented by a translation of some n-th root of unity. For odd n, we use a translation of some $2n$-th root of unity for the same purpose, noting in this case the roots of unity alternate their exponent (between odd and even) with the orientation of the underlying n-gon as the path of edge-sharing n-gons is traversed (see Figure 12).

Odd n-gons, with minimal 6-cycles and a properly oriented[1] n-gon at the origin, must satisfy

$$\sum_{i=1}^{3} \zeta_{2n}^{2\alpha_i} + \sum_{i=1}^{3} \zeta_{2n}^{2\beta_i+1} = 0$$

for integers α_i, β_i, where $\zeta_{2n} = e^{2\pi i/2n}$. The lack of asymmetry in the computational results, and the facts that $\zeta_{2n}^{n} = -1$ and $\zeta_{2n}^{2a} = \zeta_n^a$ lead to the following conjecture.

Conjecture 1 *For n odd and $\zeta_n = e^{2\pi i/n}$,*

$$\zeta_n^{a_1} + \zeta_n^{a_2} + \zeta_n^{a_3} = \zeta_n^{b_1} + \zeta_n^{b_2} + \zeta_n^{b_3}$$

if and only if either

i. $\zeta_n^{a_1} = \zeta_n^{b_i}$ for some $i \in \{1, 2, 3\}$, or

[1]In this section we change proper orientation to mean "left-pointing" and "right-pointing" n-gons.

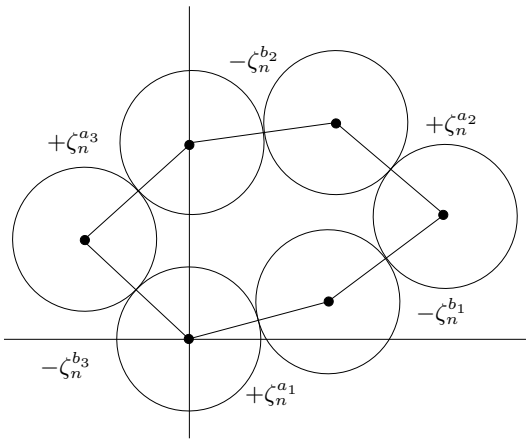

Figure 12: Roots of unity joining centres of n-gons in a 6-cycle

ii. $\sum_{i=1}^{3} \zeta_n^{a_i} = 0$.

There is a correspondence between the symmetry types of convex 6-cycles and the conjecture shown in the table below. Proof of the above conjecture, at least for the case of

symmetry	$\{\{\zeta_n^{a_1}, \zeta_n^{a_2}, \zeta_n^{a_3}\}\} = \{\{\zeta_n^{b_1}, \zeta_n^{b_2}, \zeta_n^{b_3}\}\}$	$\sum_{i=1}^{3} \zeta_n^{a_i} = 0$
2	True	False
3	False	True
6	True	True

all prime n greater than 6, relies on the properties of cyclotomic polynomials. Since this is completely subsumed by the work in the next section, we omit it.

2.10 Classification of minimal 6-cycles

So far, simple arguments have allowed us to firstly, show that the minimal cycles for n-gons are of length 3, 4, or 6, depending on the residue class of n modulo 6, and secondly, classify the minimal cycles of length 3 or 4. However, there seems to be no simple argument that allows us to classify the minimal 6-cycles.

In this section, as a first step towards a classification of minimal 6-cycles, we use arguments in cyclotomic rings to characterize all of the solutions of the equation

$$\zeta_n^{e_1} + \zeta_n^{e_2} + \zeta_n^{e_3} = \zeta_n^{e_4} + \zeta_n^{e_5} + \zeta_n^{e_6}, \tag{8}$$

where ζ_n denotes a primitive n-th root of unity for any natural number n.

Once the choices for the 6-tuple $(e_1, e_2, e_3, e_4, e_5, e_6)$ are classified, the question of which 6-tuples map to 6-cycles remains. We will address these geometric issues in a separate section. The solutions to the above equation are determined by the primes which divide

n. We begin with two simple lemmas, the first of which we will need to generalize in order to describe the solutions to equation (8).

Lemma 1 *Let n be an odd natural number, and suppose that*

$$\zeta_n^{e_1} = (-1)^w \zeta_n^{e_2},$$

where $w = 0, 1$ and $0 \le e_1, e_2 < n$. Then $w = 0$ and $e_2 = e_1$.

Proof. If $w = 1$, then the multiplicative group of odd order n generated by ζ_n contains the element -1, which has order 2. Therefore $w = 0$. Since ζ_n has order n, we have $e_2 \equiv e_1 \pmod{n}$. Since $0 \le e_1, e_2 < n$, we must have $e_2 = e_1$. □

Lemma 2 *Let p be an odd prime, and let s be odd and coprime to p. The minimal polynomial of a complex primitive p^{k+1}-th root of unity over the ring $\mathbb{Z}[\zeta_s]$ is the polynomial*

$$f(x) = 1 + x^{p^k} + x^{2p^k} + \cdots + x^{(p-1)p^k}.$$

Proof. Let $\omega := \zeta_{p^{k+1}}$ and let $m(x)$ denote the minimum polynomial of ω over $\mathbb{Z}[\zeta_s]$. Notice that $f(\omega)$ is the sum of the complex p-th roots of unity, so $f(\omega) = 0$. Therefore $m(x)$ divides $f(x)$. Moreover, since $f(x)$ is monic, it is sufficient to show that $m(x)$ and $f(x)$ have the same degree.

Now, for any ring R, the minimum polynomial $m(x)$ of ω over R is

$$\prod_{\alpha} (x - \alpha(\omega)),$$

where α ranges over the automorphisms of the ring $R[\omega]$ which fix ω. Since s is coprime to p, the ring $R[\omega]$ is $\mathbb{Z}[\omega^{1/s}]$ when $R = \mathbb{Z}[\zeta_s]$. In this case, each automorphism which fixes ω corresponds to an element $\omega^i = \alpha(\omega)$, where $i \in \{1, 2, \ldots, p^{k+1} - 1\}$ is coprime to p. Consequently, $m(x)$ has degree $(p-1)p^k = \deg(f)$. □

We now prove a substantial generalization of Lemma 1.

Lemma 3 *Let u and v be nonnegative integers, and let n be an odd natural number. Suppose that, for $w = 0$ or 1,*

$$\zeta_n^{e_1} + \zeta_n^{e_2} + \cdots + \zeta_n^{e_u} = (-1)^w (\zeta_n^{e_{u+1}} + \zeta_n^{e_{u+2}} + \cdots + \zeta_n^{e_{u+v}}). \tag{9}$$

If n is 1 or a product of primes exceeding $u + \frac{v}{2}$ and $v + \frac{u}{2}$, then either

1. *we have $w = 0$ and $\{\{e_1, e_2, \ldots, e_u\}\}$ equals $\{\{e_{u+1}, e_{u+2}, \ldots, e_{u+v}\}\}$ as multisets, or*
2. *$u + v$ is an odd prime dividing n, and $w = 1$.*

Proof. We prove this by induction on the number of primes dividing n, proving the inductive step and the initial cases at the same time. Let p be the smallest prime dividing $n = sp^{k+1}$, where s is coprime to p and $k \geq 0$. The initial case is when $s = 1$ and n is a prime power, while the inductive step is when $s > 1$ and n has at least two distinct prime divisors.

Note that $\zeta_n^{e_i}$ can be uniquely written in the form $\zeta_s^{f_i}\zeta_{p^{k+1}}^{g_i}$, where $0 \leq f_i < s$, and $0 \leq g_i < p^{k+1}$. Then (9) becomes

$$\sum_{j=1}^{u} \zeta_s^{f_j}\zeta_{p^{k+1}}^{g_j} = \sum_{j=u+1}^{u+v} \zeta_s^{f_j}\zeta_{p^{k+1}}^{g_j}. \tag{10}$$

By Lemma 2, there exists a polynomial $A(x)$ over the ring $\mathbb{Z}[\zeta_s]$ of degree at most p^k such that

$$\sum_{j=1}^{u} \zeta_s^{f_j} x^{g_j} = \sum_{j=u+1}^{u+v} \zeta_s^{f_j} x^{g_j} + A(x) \sum_{j=0}^{p-1} \left(x^{p^k}\right)^j. \tag{11}$$

Since $\deg(A) < p^k$, the number of distinct exponents of x arising when the product $A(x)(1 + x^{p^k} + \cdots + x^{(p-1)p^k})$ is expanded and collected with respect to x is ap, where a is the number of terms in the expanded and collected form of $A(x)$. Since these exponents must be matched by the exponents $g_1, g_2, \ldots, g_{u+v}$, and since $u + v < \frac{4}{3}p < 2p$, we must have $a = 0$ or 1.

We show that if $a = 1$ then $p = u + v$ is an odd prime dividing n and $w = 1$. If $a = 1$, then we have

$$(u + v)/2 < p \leq (u + v). \tag{12}$$

Since $(u + v)/2 < p$, there must be one exponent g_{i_0} which is distinct from the other exponents g_j. Therefore, we must have $A(x) = \pm\zeta_s^f x^t$ for some f and t. Consider two cases: $w = 0$ and $w = 1$. If $w = 0$, then (11) becomes

$$\sum_{j=1}^{u} \zeta_s^{f_j} x^{g_j} = \sum_{j=u+1}^{u+v} \zeta_s^{f_j} x^{g_j} \pm \zeta_s^f x^t \sum_{j=0}^{p-1} \left(x^{p^k}\right)^j. \tag{13}$$

Indeed, since $u + \frac{v}{2} < p$ and $v + \frac{u}{2} < p$, there are $i_0 \in \{1, 2, \ldots, u\}$ and $j_0 \in \{u + 1, u + 2, \ldots, u + v\}$ such that $g_{i_0} \neq g_j$ for all $j \neq i_0$, and $g_{j_0} \neq g_i$ for all $i \neq j_0$. But then

$$\zeta_s^{f_{i_0}} = \pm\zeta_s^f = -\zeta_s^{f_{j_0}},$$

which is impossible, by Lemma 1. This argument applies equally well when $s = 1$ (an initial case) and when $s > 1$ (the inductive step).

Now consider the case $w = 1$: (11) becomes

$$\sum_{j=1}^{u+v} \zeta_s^{f_j} x^{g_j} = \zeta_s^f x^t \sum_{j=0}^{p-1} \left(x^{p^k}\right)^j. \tag{14}$$

We now have two cases: $p = u+v$, and $p < u+v$. In the latter case, there are z exponents $g_{i_1} = g_{i_2} = \cdots = g_{i_z}$ where $1 \le z-1 \le u+v-p < p/3$, such that $g_j = g_{i_1}$ if and only if $j = i_1, i_2, \ldots, i_z$. In this case, (14) implies that

$$\sum_{j=1}^{z} \zeta_s^{f_{i_j}} = \zeta_s^f \,.$$

If $s = 1$ (i.e., $n = p^{k+1}$ has just one prime divisor), we have $z = 1$—a contradiction. If $s > 1$, then, since (a) all primes dividing s exceed p and hence exceed $p/3+1$, (b) s has one fewer prime divisors than n, and (c) $z > 1$, we have a contradiction by induction. Therefore if $a = 1$, we must have that $p = u+v$ is an odd prime. Moreover, $\zeta_s^{f_i} = \zeta_s^f$ for all $i = 1, 2, \ldots, u+v$, and the multiset $\{\{g_1, g_2, \ldots, g_{u+v}\}\} = \{\{t, t+p^k, \ldots, t+(p-1)p^k\}\}$. Consequently, $p = u+v$ is an odd prime dividing n, and $w = 1$. So if $a = 1$, the second part of the lemma applies.

Now consider the case where $a = 0$. In this case, (11) yields

$$\sum_{j=1}^{u} \zeta_s^{f_j} x^{g_j} = (-1)^w \sum_{j=u+1}^{u+v} \zeta_s^{f_j} x^{g_j} \tag{15}$$

Now when $s = 1$ (an initial case), we have $u = (-1)^w v$, and

$$\{\{g_1, g_2, \ldots, g_u\}\} = \{\{g_{u+1}, g_{u+2}, \ldots, g_{u+v}\}\}.$$

Moreover, $e_i = g_i$. So the lemma holds. This completes the proof of the initial cases. Completion of the proof of the inductive step remains.

When $s > 1$, s is the product of primes exceeding $u + v/2$ and $v + u/2$, so $s > v$. Setting $x = \zeta_s^{-c}$ in (15) yields, for all $c = 0, 1, \ldots, s-1$,

$$\sum_{j=1}^{u} \zeta_s^{f_j - cg_j} = (-1)^w \sum_{j=u+1}^{u+v} \zeta_s^{f_j - cg_j} \tag{16}$$

By induction on the number of prime divisors, we have $w = 0$ and

$$\{\{f_1 - cg_1, f_2 - cg_2, \ldots, f_u - cg_u\}\} \\ = \{\{f_{u+1} - cg_{u+1}, f_{u+2} - cg_{u+2}, \ldots, f_{u+v} - cg_{u+v}\}\} \,.$$

Since $s > v$, the pigeonhole principle implies that there is a $j_0 \in \{u+1, u+2, \ldots, u+v\}$ and $c_1 \ne c_2$ such that

$$f_1 - c_1 g_1 = f_{j_0} - c_1 g_{j_0} \qquad \text{and} \qquad f_1 - c_2 g_1 = f_{j_0} - c_2 g_{j_0} \,.$$

Thus $f_{j_0} = f_1$ and $g_{j_0} = g_1$, and (16) becomes (after swapping the indexes $u+1$ and j_0 if necessary)

$$\sum_{j=2}^{u} \zeta_s^{f_j - cg_j} = \sum_{j=u+2}^{u+v} \zeta_s^{f_j - cg_j} \,. \tag{17}$$

Applying the argument for (f_1, g_1) in turn for the pairs $(f_2, g_2), \ldots, (f_u, g_u)$, we conclude that

$$\{\{(f_1, g_1), (f_2, g_2), \ldots, (f_u, g_u)\}\} \\ = \{\{(f_{u+1}, g_{u+1}), (f_{u+2}, g_{u+2}), \ldots, (f_{u+v}, g_{u+v})\}\},$$

and this implies that $\{\{e_1, e_2, \ldots, e_u\}\} = \{\{e_{u+1}, e_{u+2}, \ldots, e_{u+v}\}\}$. This completes the proof of the inductive step, and hence the lemma. □

We are now ready to consider (8).

Theorem 2.2 *Let n be an odd natural number. Then*

1. *Suppose that $n \equiv \pm 1 \pmod 6$. For $0 \le e_1, e_2, e_3, e_4, e_5, e_6 < n$ we have (8) iff $\{\{e_1, e_2, e_3\}\} = \{\{e_4, e_5, e_6\}\}$.*

2. *Suppose that $n \equiv 3 \pmod 6$. Write $n = s3^{k+1}$, where $k \ge 0$, and s is coprime to 3. For $0 \le e_1, e_2, e_3, e_4, e_5, e_6 < n$ we have (8) iff (upon relabelling if necessary) one of the following holds*

   (a) *$\zeta_n^{e_i} = \zeta_s^{f_i}\zeta_{3^{k+1}}^{g_i}$, where $0 \le f_i < s$, $0 \le g_i < 3^{k+1}$, and $f_1 = f_2 = f_3$, $f_4 = f_5 = f_6$, $f_1 \ne f_4$, $g_1 = g_2 - 3^k = g_3 - 2 \cdot 3^k$, $g_4 = g_5 - 3^k = g_6 - 2 \cdot 3^k$,*

   (b) *$\{\{e_1, e_2, e_3\}\} = \{\{e_4, e_5, e_6\}\}$.*

Proof. 1. In this case, $n = 1$ or is a product of primes exceeding five, therefore Lemma 3 applies with $u = v = 3$. Furthermore, since $u + v = 6$ is not prime, only part 1 of the conclusion of the lemma is possible. Thus $\{\{e_1, e_2, e_3\}\} = \{\{e_4, e_5, e_6\}\}$.

2. Write $n = s3^{k+1}$ where $k \ge 0$ and s is coprime to 3. We can write $\zeta_n^{e_i}$ in the form $\zeta_s^{f_i}\zeta_{3^k}^{g_i}$, where $0 \le f_i < s$, and $0 \le g_i < 3^{k+1}$ are uniquely determined by e_i. Equation (8) then becomes

$$\sum_{j=1}^{3} \zeta_s^{f_j}\zeta_{3^{k+1}}^{g_j} = \sum_{j=4}^{6} \zeta_s^{f_j}\zeta_{3^{k+1}}^{g_j}.$$

By Lemma 2, the minimum polynomial of $\zeta_{3^{k+1}}$ is $1 + x^{3^k} + x^{2\cdot 3^k}$, so we have

$$\sum_{j=1}^{3} \zeta_s^{f_j} x^{g_j} = \sum_{j=4}^{6} \zeta_s^{f_j} x^{g_j} + A(x) \sum_{j=0}^{2} \left(x^{3^k}\right)^j, \tag{18}$$

where $\deg(A) < 3^k$. Consequently, we have three possible forms for $A(x)$:

I. $A(x) = 0$

II. $A(x) = bx^t$,where $b \ne 0$ is in $\mathbb{Z}[\zeta_s]$, and $0 \le t < 3^k$,

III. $A(x) = b_1x^{t_1} + b_2x^{t_2}$, where $b_1, b_2 \ne 0$ are in $\mathbb{Z}[\zeta_s]$, and $0 \le t_1 \ne t_2 < 3^k$.

We consider these in reverse order.

III. In this case, we have $\{g_1, g_2, g_3, g_4, g_5, g_6\} = \{t_1, t_1+3^k, t_1+3^{2\cdot 3^k}, t_2, t_2+3^k, t_2+3^{2\cdot 3^k}\}$. Relabelling if necessary, we have $g_1 = t_1$, and so $b_1 = \zeta_s^{f_1}$. By part 1, in order to get full cancellation, we must then have $\{g_2, g_3\} = \{t_1 + 3^k, t_1 + 3^{2\cdot 3^k}\}$, $f_3 = f_2 = f_1$, $b_2 = \zeta_s^{f_4}$, $f_6 = f_5 = f_4$, and $\{g_4, g_5, g_6\} = \{t_2, t_2 + 3^k, t_2 + 3^{2\cdot 3^k}\}$. Finally, since $b_1 \neq b_2$, we have $f_1 \neq f_4$.

II. Let a_1 denote the number of indexes i such that $g_i = t_1$, let a_2 denote the number of indexes i such that $g_i = t_1 + 3^k$, and let a_3 denote the number of indexes i such that $g_i = t_1 + 2 \cdot 3^k$. Now $1 \leq a_1, a_2, a_3$, and $a_1 + a_2 + a_3 \leq 6$. Let $a = 6 - a_1 - a_2 - a_3$: then $a \leq 3$ and $a \neq 1$. Now, if $a = 3$ then for some h_1, h_2, h_3, we have

$$\zeta_s^{h_1} \pm \zeta_s^{h_2} \pm \zeta_s^{h_3} = 0\,. \tag{19}$$

Since 5 is the largest prime dividing s, Lemma 3 implies that this is not possible, so either $a = 0$ or 2. If $a = 2$, then $\{\{a_1, a_2, a_3\}\} = \{\{1, 1, 2\}\}$. Hence, permuting the exponents $g_1, g_2, \ldots, g_6$ if necessary, $b = \zeta_s^{f_1}$, and then (since a_1, a_2 or a_3 equals 2), full cancellation in (18) implies the impossible condition (19). So $a = 0$, and the possibilities for $\{\{a_1, a_2, a_3\}\}$ are $\{\{1, 1, 4\}\}, \{\{1, 2, 3\}\}$ and $\{\{2, 2, 2\}\}$.

If $\{\{a_1, a_2, a_3\}\} = \{\{1, 1, 4\}\}$, then $b = \zeta_s^{f_1}$ and we have

$$\zeta_s^{h_1} \pm \zeta_s^{h_2} \pm \zeta_s^{h_3} \pm \zeta_s^{h_4} = \zeta_s^{f_1}\,.$$

Now if $\{\{a_1, a_2, a_3\}\} = \{\{1, 2, 3\}\}$, then $b = \zeta_s^{f_1}$ and we have

$$\pm\zeta_s^{h_1} \pm \zeta_s^{h_2} = \zeta_s^{f_1}\,.$$

Since the smallest prime dividing s is five, Lemma 3 implies that both of these identities are impossible, so $\{\{a_1, a_2, a_3\}\} = \{\{2, 2, 2\}\}$. In this case, there are indexes $i_0 \in \{g_1, g_2, g_3\}$ and $j_0 \in \{g_4, g_5, g_6\}$ such that $g_{i_0} = g_{j_0}$ and $g_i = g_{i_0}$ iff $i = i_0$ or j_0. So relabelling the exponents g_1, g_2, g_3 and the exponents g_4, g_5, g_6, we have $\zeta_s^{f_1} - \zeta_s^{f_4}$. Now if $g_2 = g_3$, then

$$\zeta_s^{f_2} + \zeta_s^{f_3} = \zeta_s^{f_1} - \zeta_s^{f_4},$$

which, by Lemma 3, cannot happen. So, swapping g_5 and g_6 if necessary, we have $g_2 = g_5$, $g_3 = g_6$,

$$\zeta_s^{f_2} - \zeta_s^{f_5} = \zeta_s^{f_1} - \zeta_s^{f_4} \qquad \text{and} \qquad \zeta_s^{f_3} - \zeta_s^{f_6} = \zeta_s^{f_1} - \zeta_s^{f_4}\,.$$

Thus $\{\{g_1, g_2, g_3\}\} = \{\{g_4, g_5, g_6\}\} = \{\{t, t + 3^k, t + 2 \cdot 3^k\}\}$. Moreover, by Lemma 3, we must have $\{\{f_2, f_4\}\} = \{\{f_1, f_5\}\}$ and $\{\{f_3, f_4\}\} = \{\{f_1, f_6\}\}$. Now since $b \neq 0$, we have $f_1 = f_2 = f_3$, $f_4 = f_5 = f_6$, and $f_1 \neq f_4$.

I. We have

$$\sum_{j=1}^{3} \zeta_s^{f_j} x^{g_j} = \sum_{j=4}^{6} \zeta_s^{f_j} x^{g_j}\,. \tag{20}$$

Partition the set $\{1, 2, 3, 4, 5, 6\}$ into disjoint subsets so that i and j are in the same subset if and only if $g_i = g_j$. Then by Lemma 3, each subset must have even order. Moreover, for each such subset S of order $2a$, we have $\{\{f_i | i \in S \cap \{1, 2, 3\}\}\} = \{\{f_j | j \in S \cap \{4, 5, 6\}\}\}$. Consequently, $\{\{f_1, f_2, f_3\}\} = \{\{f_4, f_5, f_6\}\}$. □

Corollary 2.3 *Let $n \equiv \pm 1 \pmod 6$ be an odd integer greater than one. Then all 6-cycles of n-gons have at least C_2 symmetry.*

Proof. Since $\{\{e_1, e_2, e_3\}\} = \{\{e_4, e_5, e_6\}\}$, we may suppose the 6-sided polygon with vertices equal to the centers of the n-gons has opposite sides which are parallel to each other. □

2.11 Symmetries of 6-cycles

We continue to consider 6-cycles constructed from near-tilings of odd n-gons and use the arguments of the previous section to reveal more about their symmetries. Arbitrary equilateral hexagons (see Figure 13) can have only the following types of non-trivial rigid, planar symmetries:

- a rotation group C_2 iff $a = d$, $b = e$, $c = f$ and at most one pair of a, b, c are equal,
- a rotation group C_3 iff $a = c = e$, $b = d = f$ and $a \neq b$, or
- a rotation group C_6 iff $a = b = c = d = e = f$.

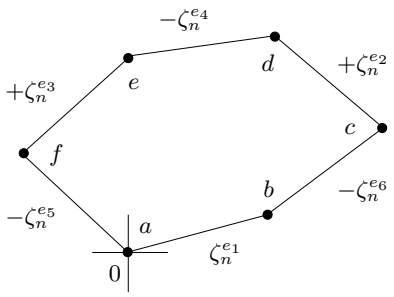

Figure 13: Roots of unity joining centres of odd n-gons in a 6-cycle

If we constrain the sides of the hexagon to be sums of alternating positive and negative n-th roots of unity, then since $\arg(\zeta_n^{e_i}) = 2\pi e_i/n + 2k_i\pi$ and $\arg(-\zeta_n^{e_i}) = (2e_i+n)\pi/n + 2l_i\pi$,

$$a = \frac{2\pi}{n}(e_5 - e_1) + 2k_a\pi, \qquad b = \frac{2\pi}{n}(e_1 - e_6) + 2k_b\pi,$$
$$c = \frac{2\pi}{n}(e_6 - e_2) + 2k_c\pi, \qquad d = \frac{2\pi}{n}(e_2 - e_4) + 2k_d\pi,$$
$$e = \frac{2\pi}{n}(e_4 - e_3) + 2k_e\pi, \qquad f = \frac{2\pi}{n}(e_3 - e_5) + 2k_f\pi.$$

In particular, this means that the symmetry conditions above can be translated into constraints on the exponents of the roots of unity.

First consider the case of $n \equiv \pm 1 \pmod 6$. For the C_3 symmetry,

$$\begin{aligned} a = c = e &\implies e_5 - e_1 \equiv e_6 - e_2 \equiv e_4 - e_3 \pmod n \\ b = d = f &\implies e_1 - e_6 \equiv e_2 - e_4 \equiv e_3 - e_5 \pmod n \end{aligned}$$

which upon summation leads to $3(e_5 - e_6) \equiv 0 \pmod n$. Since $a \neq b$ for this symmetry, or $e_5 \neq e_6$, we conclude that n is divisible by 3. This contradiction shows that 6-cycles constructed from n-gons in this case cannot have 3-fold symmetry. This, with Corollary 2.3, proves that such 6-cycles have exactly C_2 symmetry.

Next consider the case $n \equiv 3 \pmod 6$. The following is an equivalent criterion for C_3 symmetry. A 6-cycle has C_3 symmetry when the alternate edges form (via parallel transport) an equilateral triangle:

$$\zeta_n^{e_1} + \zeta_n^{e_2} + \zeta_n^{e_3} = 0.$$

Conversely, if $\sum_{i=1}^{3} \zeta_n^{e_i} = 0$, then $\sum_{i=4}^{6} \zeta_n^{e_i} = 0$, since we are assuming that equation 8 holds. Thus we have two equilateral triangles, the sides of which can be interlaced to form a 6-cycle with at least C_3 symmetry (see Figure 14). Notice that part (a) of the second

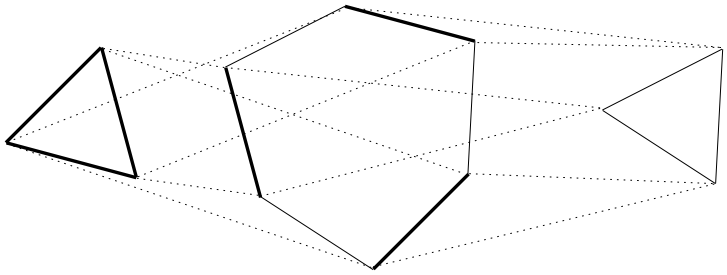

Figure 14: A 6-cycle with C_3 symmetry

condition in Theorem 2.2 implies that

$$\begin{aligned} \sum_{j=1}^{3} \zeta_n^{e_j} &= \sum_{j=0}^{2} \zeta_s^{f_1} \zeta_{3^{k+1}}^{g_1 + j3^k} \\ &= \zeta_s^{f_1} \zeta_{3^{k+1}}^{g_1} \sum_{j=0}^{2} \zeta_{3^{k+1}}^{j3^k} \end{aligned}$$

which is zero by Lemma 2. Furthermore, by definition, $e_i = f_i 3^{k+1} + g_i s$, and so if $e_1 = e_4$, then

$$e_1 = f_1 3^{k+1} + g_1 s = f_4 3^{k+1} + g_4 s = e_4,$$

or equivalently, $f_1 \equiv f_4 \pmod s$. Since $f_1 \neq f_4$, we can infer $e_1 \neq e_4$. Similarly, $e_1 \neq e_5$ and $e_1 \neq e_6$. Thus $\{\{e_1, e_2, e_3\}\} \neq \{\{e_4, e_5, e_6\}\}$ which implies there is no C_2 symmetry in this subcase, only C_3 symmetry.

In the final subcase of $n \equiv 3 \pmod 6$, namely part (b) of the second part of Theorem 2.2, we have $\{\{e_1, e_2, e_3\}\} = \{\{e_4, e_5, e_6\}\}$. This can be split into two possible subcases, depending on whether or not $\sum_{j=1}^{3} \zeta_n^{e_j} = 0$. If $\{\{e_1, e_2, e_3\}\} = \{\{e_4, e_5, e_6\}\}$, it is clear that opposite sides of the 6-cycle must be parallel, giving us at least C_2 symmetry. If $\sum_{j=1}^{3} \zeta_n^{e_j} \neq 0$ there is only C_2 symmetry but if $\sum_{j=1}^{3} \zeta_n^{e_j} = 0$, we also get C_3 symmetry.

Combining all of the above arguments proves the following.

Theorem 2.4 *If n is odd, then the minimal 6-cycles have the following symmetries.*

- C_2 *if* $n \equiv \pm 1 \pmod 6$.
- C_3 *if* $n \equiv 3 \pmod 6$ *and* $\{\{e_1, e_2, e_3\}\} \neq \{\{e_4, e_5, e_6\}\}$.
- *If* $n \equiv 3 \pmod 6$ *and* $\{\{e_1, e_2, e_3\}\} = \{\{e_4, e_5, e_6\}\}$, *either*
  - C_2 *if* $\sum_{j=1}^{3} \zeta_n^{e_j} \neq 0$, *or*
  - C_6 *if* $\sum_{j=1}^{3} \zeta_n^{e_j} = 0$.

We now wish to use this theorem to prove the experimentally determined formula for $N_6(n)$ at the end of section 2.8.

First, in the $n \equiv \pm 1 \pmod 6$ case, we can use equation 6 and Theorem 2.4 to argue that the number of interior edges from one shared edge to the next is given by

$$(I_1, I_2, I_3, I_4, I_5, I_6) = (k, l, n-k-l-3, k, l, n-k-l-3)\,,$$

where k and l are integers. Furthermore, repeated sets of parameters are avoided by ensuring that k corresponds to the smallest allowable internal angle, while l corresponds to the largest allowable internal angle. Thus

$$\frac{\pi}{3} < (k+1)\frac{2\pi}{n} < \frac{2\pi}{3} \qquad \text{and} \qquad \frac{2\pi}{3} < (l+1)\frac{2\pi}{n} < \pi.$$

So

$$\frac{n}{6} - 1 < k < \frac{n}{3} - 1 \qquad \text{and} \qquad \frac{n}{3} - 1 < l < \frac{n}{2} - 1.$$

While one of these parameters, k say, can be allowed to range freely over the interval, they are not both free since I_3 must correspond to the middle-sized interior angle. That is,

$$(k+1)\frac{2\pi}{n} \leq (n-k-l-2)\frac{2\pi}{n} \leq (l+1)\frac{2\pi}{n},$$

or equivalently,

$$\frac{n-k-3}{2} \leq l \leq n - 2k - 3.$$

Combining the two constraints on l and observing that $(n-k-3)/2 \geq n/3 - 1$ gives us

$$\frac{n-k-3}{2} \leq l \leq \min\left\{\frac{n}{2} - 1, n - 2k - 3\right\}.$$

Now we simply want to count the number of lattice points inside the region of the kl-plane defined by the above constraints. Since $n/2 - 1 = n - 2k - 3$ if $k = n/4 - 1$, the k range can be split into two pieces over which the upper bound for l swaps. To ease the computation, replace k and l by $k' = k + 1$ and $l' = l + 1$, which converts the region into

$$\frac{n}{6} < k' < \frac{n}{3} \qquad \text{and} \qquad \frac{n - k'}{2} \leq l' \leq \min\left\{\frac{n}{2}, n - 2k'\right\},$$

(see Figure 15). Notice that the area of the grey region is $n^2/72$, which is asymptotically

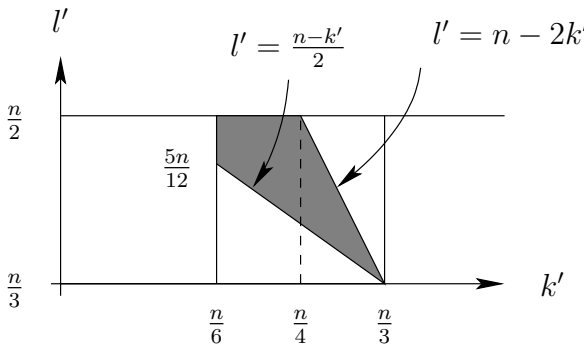

Figure 15: Region in the $k'l'$-plane corresponding to distinct 6-cycles

the same as that given by the experimental formula for $N_6(n)$.

We compute the exact result in the case $n = 24m - 1$. Recall Pick's theorem: a lattice polygon with I interior points and B boundary points has area

$$I + B/2 - 1.$$

To apply this we find the vertices of the convex hull of the lattice points inside, or on, the quadrilateral of Figure 16. This causes complications only on the lower boundary. For example, we compute the coordinates of the lattice point C to the left of $k' = \frac{n}{4}$ and

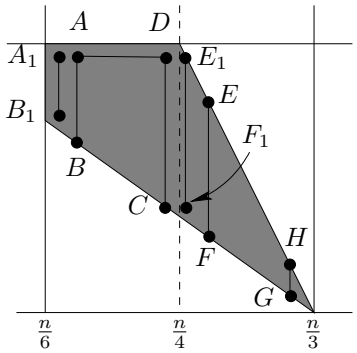

Figure 16: Extrema of convex hull of lattice points in $k'l'$-plane

above or on $l' = \frac{n-k'}{2}$:

$$\begin{aligned}\left(\left\lfloor\frac{n}{4}\right\rfloor, \left\lceil\frac{n-k'}{2}\right\rceil\right) &= \left(\left\lfloor\frac{24m-1}{4}\right\rfloor, \left\lceil\frac{24m-1-k'}{2}\right\rceil\right)\\ &= \left(6m-1, \left\lceil\frac{24m-1-(6m-1)}{2}\right\rceil\right)\\ &= (6m-1, 9m).\end{aligned}$$

The 12 points are

$$\begin{aligned} A_1 &= (4m, 12m-1) & B_1 &= (4m, 10m)\\ A &= (4m+1, 12m-1) & B &= (4m+1, 10m-1)\\ C &= (6m-1, 9m) & D &= (6m-1, 12m-1)\\ E_1 &= (6m, 12m-1) & F_1 &= (6m, 9m)\\ E &= (6m+1, 12m-3) & F &= (6m+1, 9m-1)\\ G &= (8m-1, 8m) & H &= (8m-1, 8m+1). \end{aligned}$$

The number of lattice points in the grey quadrilateral is

$$N_6(24m-1) = \text{pts}(A_1B_1) + \text{pts}(ABCD) + \text{pts}(E_1F_1) + \text{pts}(EFGH),$$

where pts() denotes the number of lattice points in and on the boundary of the (possibly degenerate) polygon joining those points. We compute these in turn using Pick's theorem and the trapezoid area formula or by simply counting them. So

$$\begin{aligned}\text{pts}(A_1B_1) &= (12m-1) - (10m) + 1 = 2m\\ \text{pts}(ABCD) &= \frac{1}{2}(5m-1)(2m-2) + \frac{1}{2}(8m-4) + 1 = 5m^2 - 2m\\ \text{pts}(E_1F_1) &= (12m-1) - (9m) + 1 = 3m\\ \text{pts}(EFGH) &= \frac{1}{2}(3m-1)(2m-2) + \frac{1}{2}(6m-4) + 1 = 3m^2 - m.\end{aligned}$$

So

$$N_6(24m-1) = 8m^2 + 2m,$$

which confirms the experimental formula in this case. The remaining seven cases when $n \equiv 1, 5, 7, 11, 13, 17, 19 \pmod{24}$ are similar.

Now consider the $n \equiv 3 \pmod 6$ case, which is different from the previous one, in that all three symmetry groups must be dealt with. First, if we assume that $n = 6N+3$, then the C_3 symmetry and equation (6) force the interior edge counts to be

$$(I_1, I_2, I_3, I_4, I_5, I_6) = (k, 4N-k, k, 4N-k, k, 4N-k)\,.$$

Since the angle corresponding to I_2 does not restrict us in any way, there is only one free parameter k, which is constrained by

$$\frac{\pi}{3} < (k+1)\frac{2\pi}{n} < \frac{2\pi}{3},$$

which immediately provides us with the lattice point count:

$$N_{6,C_3}(n) = \left\lfloor \frac{n}{3} \right\rfloor - \left\lceil \frac{n}{6} \right\rceil = \frac{n-3}{6}.$$

We combine the remaining two cases of C_2 or C_6 symmetry. Equation (6) implies that

$$(I_1, I_2, I_3, I_4, I_5, I_6) = (k, l, n-k-l-3, k, l, n-k-l-3)\,,$$

where

$$\frac{n}{6} < k' \le \frac{n}{3} \qquad \text{and} \qquad \frac{n-k'}{2} \le l' \le \min\left\{\frac{n}{2}, n-2k'\right\},$$

for $k' = k+1$ and $l' = l+1$. We allow equality in the upper bound for k' to account for the regular hexagon. As before, we compute the exact count of the lattice points in this region for a specific case, $n = 24m+3$. This time we have one quadrilateral and a segment to the left of the central line $k' = \frac{n}{4}$ and one triangle to the right of the central line.

The 9 extreme points are

$$\begin{aligned} A &= (4m+1, 12m+1) & B &= (4m+1, 10m+1) \\ C &= (6m-1, 9m+2) & D &= (6m-1, 12m+1) \\ C_1 &= (6m, 9m+2) & D_1 &= (6m, 12m+1) \\ E &= (6m+1, 12m+1) & F &= (6m+1, 9m+1) \\ G &= (8m+1, 8m+1). \end{aligned}$$

The number of lattice points in the appropriate region is

$$N_{6,C_2,C_6}(24m+3) = \mathrm{pts}(ABCD) + \mathrm{pts}(C_1D_1) + \mathrm{pts}(EFG).$$

Hence

$$\begin{aligned} \mathrm{pts}(ABCD) &= \frac{1}{2}(5m-1)(2m-2) + \frac{1}{2}(8m-4) + 1 = 5m^2 - 2m \\ \mathrm{pts}(C_1D_1) &= (12m+1) - (9m+2) + 1 = 3m \\ \mathrm{pts}(EFG) &= \frac{1}{2}(3m)(2m) + \frac{1}{2}(6m) + 1 = 3m^2 + 3m + 1. \end{aligned}$$

So

$$\begin{aligned} N_6(24m+3) &= N_{6,C_2,C_6}(24m+3) + N_{6,C_3}(24m+3) \\ &= (8m^2 + 4m + 1) + (4m) \\ &= 8m^2 + 8m + 1, \end{aligned}$$

which is identical to the conjectural formula. As before, the other three cases $n \equiv 9, 15, 21 \pmod{24}$ are similar. All this proves the the formula for $N_6(n)$ in Theorem 2.1 at the end of section 2.8.

2.12 Near-tilings with minimal cycles

When we attempt to produce near-tilings of the plane using only minimal cycles, there are three cases to consider: the 3-cycle, 4-cycle and 6-cycle.

Recall that the 3-cycle tiles in a rigid way, and so there is a unique near-tiling for all n-gons satisfying $n \equiv 0 \pmod 6$. In fact, the underlying graph (of the centrepoint connections) is isomorphic to the equilateral triangle tiling or the lattice $\mathbb{Z} + \omega\mathbb{Z}$, where $\omega = e^{i\pi/3}$.

All polygons which satisfy $n \equiv \pm 2 \pmod 6$ have minimal cycles of length four. Apart from the square and octagon, which near-tessellate in a unique way, these 4-cycles can themselves tile in uncountably many ways. If we consider infinite strips composed of one of two orientations of the 4-cycle, labelled "0" and "1" as in Figure 17, then any doubly infinite binary sequence corresponds to such a strip. By stacking these strips, we can then

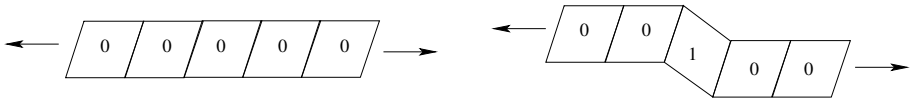

Figure 17: Uncountable 4-cycle near-tilings

tile the infinite plane in uncountably many distinct ways. Of course this hardly exhausts the possible 4-cycle near-tilings, since we can tile some rhombi in a star (e.g. Figure 18).

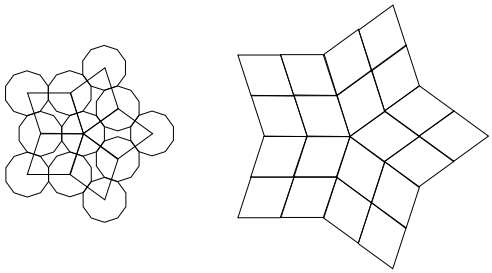

Figure 18: Star-like near-tiling of a decagon 4-cycle

Any polygon with $n \equiv 1, 3, 5 \pmod 6$ has minimal cycles of length 6. For 6-cycles, the underlying graph (see Figure 19) is not necessarily a discrete subset of the Euclidean plane, and so nodes can ultimately lie arbitrarily close to one another. This is because the vector sum $-e^{i\pi/n} + 1 + e^{i\pi(n-1)/n}$ is zero only if $n = 3$ and forms a lattice only in that case. This leads to a phenomenon of partial edge sharing (see Figure 20), which we typically exclude from consideration in this paper. As in the case of 4-cycles, a correspondence can be made between binary sequences and linear strips of 6-cycles (see Figure 21) to show that there are an uncountable number of such near-tilings.

For any such near-tiling, one can apply a process that we call the *spiral* algorithm to create a sequence of configurations. First select a particular tile, called the central tile,

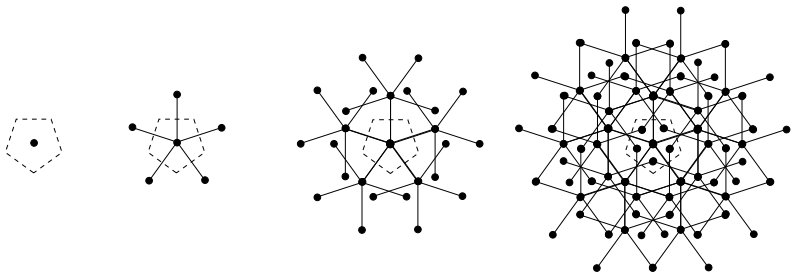

Figure 19: Pentagonal centrepoint graphs, G_1, G_2, G_3, and G_4

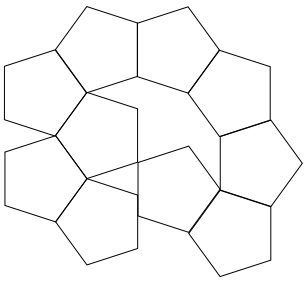

Figure 20: Partial edge sharing for 10 pentagons

and then successively choose tiles closest to the central tile, in a spiral manner, which are edge-connected to the current tile. Observe that there are two spiral algorithms (one of each orientation) for each choice of a central tile in any near-tiling. Intuitively, the spiral algorithm attempts to maximise the local edge-sharing at each stage and so is expected to provide optimal configurations for near-tilings composed only of minimal cycles.

While this was proven for the square, triangular and hexagonal tilings (see [5]), for near-tilings with holes, however, life is a little more difficult. Just because a near-tiling is made up only of 6-cycles does not mean that it is necessarily optimal. Take for example the hexagonal and decagonal near-tilings of the regular pentagon (see Figures 22, 23). The fault lines in both figures allow us to write down the recursive formulæ for the spiral algorithm applied to both near-tilings when started at the obvious central pentagon. When we compare the formulæ for the same number of pentagons, k say, we find that the decagonal near-tiling is almost always less efficient than the hexagonal near-tiling. The first point at which it requires more unit edges is for 13 pentagons, requiring 51 edges as opposed to 50. It appears that there are only a finite number of configurations for which the decagonal near-tiling produces as low an edge count as the hexagonal near-tiling (see Table 3). In fact, a comparison of all corresponding configurations for these two near-tilings up to $20,000$ tiles shows that the decagonal near-tiling is never as good as the hexagonal near-tiling for any $21 < k < 20000$.

To make headway on such problems, we assume that a near-tiling of odd n-gons is composed of only 6-cycles, of only one type, in such a way that the corresponding graph is

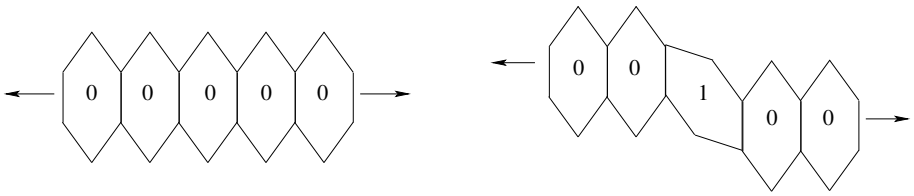

Figure 21: Uncountable 6-cycle near-tilings

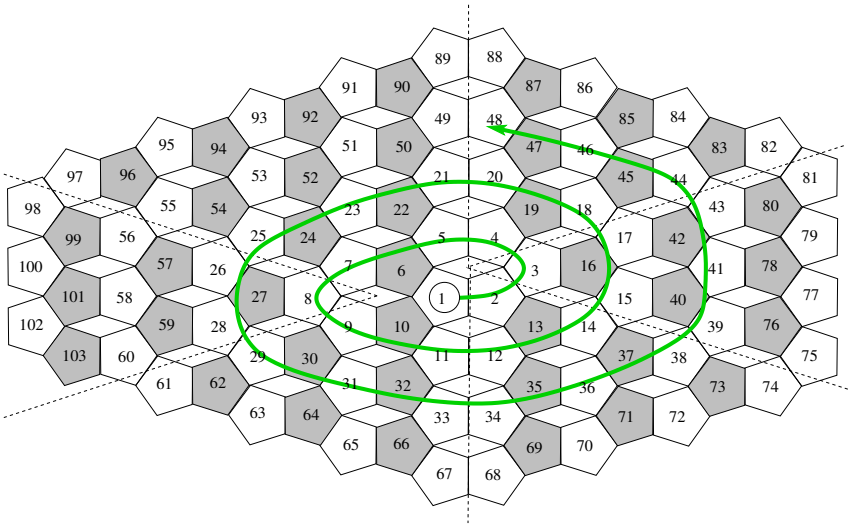

Figure 22: Hexagonal near-tiling of the regular pentagon (central pentagon: 5 edges, white pentagon: add 4 edges, grey pentagon: add 3 edges).

regular of degree 3—apart from the perimeter. Since the 6-cycles actually form a proper tiling with congruent tiles, we have concentric shells of 6-cycles around a chosen starting 6-cycle. These form a graph topologically equivalent to a finite subgraph of the regular hexagonal tiling. In this case, it is easy to determine that the number of faces in s completed concentric shells is given by

$$F(s) = 3s^2 - 3s + 1.$$

The number of faces in any annulus is simply

$$F_{\text{annulus}}(s) = F(s) - F(s-1) = 6s - 6$$

while the number of edges on a completed perimeter is

$$P(s) = 2F_{\text{annulus}}(s) + 6 = 12s - 6$$

or equivalently, $P(s+1) = P(s) + 12$. Finally, the ratio of the number of perimeter edges to the number of internal edges is smaller than $P(s)/F(s)$, which goes to 0 as s goes

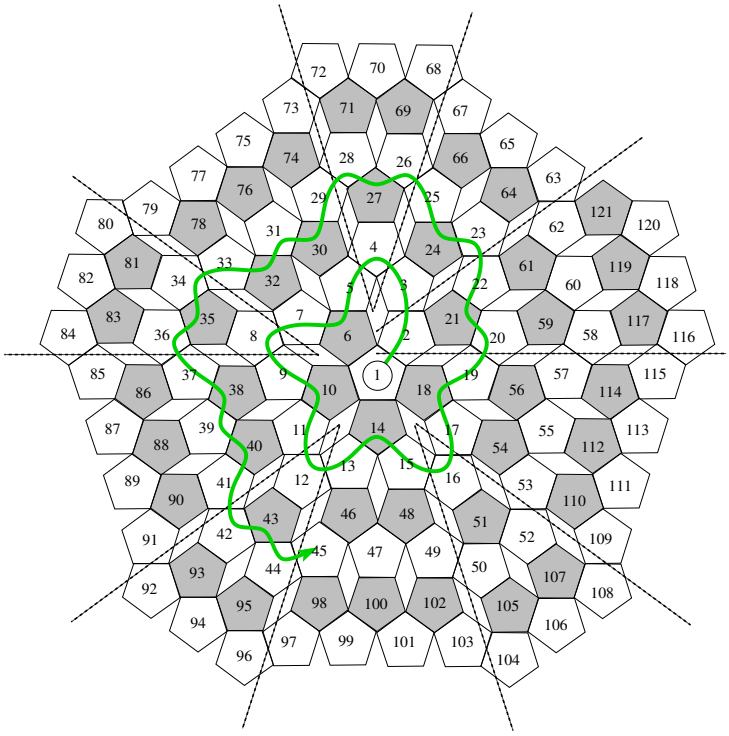

Figure 23: Decagonal near-tiling of the regular pentagon (central pentagon: 5 edges; white pentagon: add 4 edges; grey pentagon: add 3 edges).

to infinity. This implies that the spiral algorithm applied to all the uncountably many 3-regular near-tilings, described above, is asymptotically optimal. A similar argument can be used to show that the decagonal near-tiling, with a single degree 5 vertex at the centre of its corresponding graph, has

$$F(s) = 5s^2 \quad \text{and} \quad P(s) = 20s$$

for s completed shells. In particular, this means that $P(s+1) = P(s) + 20$. Hence the spiral algorithm is again asymptotically optimal for this type of tiling. Notice that both the hexagonal and decagonal near-tilings satisfy the requirement that

$$P(s+1) \leq P(s) + 2|\{\text{fault-lines}\}|$$

where the number of fault-lines is 6 for the hexagonal near-tiling and 10 for the decagonal near-tiling. To prove that the spiral algorithm is optimal, we need to show that there are a bounded number of fault lines in any such near-tiling—something we have not yet done.

3 Conclusion

While this work leads to many unanswered questions, especially in the sections on near-tilings, arguably the most important is the following:

k	decagonal	hexagonal	k	decagonal	hexagonal
1	5	5	12	47	47
2	9	9	13	51	50
3	13	13	14	54	54
4	17	17	15	58	58
5	21	21	16	62	61
6	24	24	17	66	65
7	28	28	18	69	69
8	32	32	19	73	72
9	36	36	20	77	76
10	39	39	21	80	80
11	43	43	22	84	83

Table 3: Decagonal- versus hexagonal-pentagon near-tiling spiral edge counts

Are there any near-tilings for which the spiral algorithm does not provide a minimal configuration for each k?

Similar optimisation questions can be asked of more general tiles than the regular polygons we consider. For example equilateral tiles which are not necessarily equiangular (like an 8-edge L-shaped tile) would provide an interesting test-bed of non-convex tiles that might shed some light on the above question.

Acknowledgments

The authors would like to thank Zoltán Bácskai, Bobby Compton, Henry Haselgrove, Nicholas McConnell and Robert Stingley for their many useful discussions, contributions and ideas. In particular, Henry wrote dedicated C code which extended the observations of the symmetries of 6-cycles for polygons with up to 1001 sides. He also pointed out that some of the symmetry survives even in the non-convex and overlapping 6-cycles. Robert was kind enough to provide many of the subcases of the proof of the $N_6(n)$ formula while Bobby was the first to discover the decagonal pentagon tiling as well as some of its properties.

The authors would also like to acknowledge the constructive criticism of an anonymous referee and the subsequent editorial suggestions of Leisa Condie.

References

[1] Ralph Buchholz, *Spiral Polygon Series*, School Mathematics Journal, no. 31, November 1985, University of Newcastle.

[2] J. Bornhoft, G. Brinkmann, and J. Greinus, *Pentagon-hexagon-patches with short boundaries*, European Journal of Combinatorics, vol. 24, no. 5, pp. 517-529, 2003.

[3] Branko Grünbaum, G. C. Shephard, *Tilings and Patterns*, W. H. Freeman and Co., October 1986.

[4] Thomas C. Hales, *The honeycomb structure*, Discrete and Computational Geometry, vol. 25, pp 1-22, 2001.

[5] Frank Harary and Heiko Harborth, *Extremal animals*, Journal of Combinatorics, Information and System Sciences, vol. 1, no. 1, pp 1-8, 1976.

[6] M.A. Fortes and P.I.C. Teixeira, *Minimum perimeter partitions of the plane into equal numbers of regions of two different areas*, Eur. Phys. J. E 6, pp. 133-137, 2001.

[7] Sándor Kabai, *Pentagonal Tiling around a Pentagon*, The Wolfram Demonstrations Project, `http://demonstrations.wolfram.com/PentagonalTilingAroundAPentagon/`.

[8] Y. S. Kupitz, *On the maximal number of appearances of the minimal distance among n points in the plane*, Intuitive geometry, K. Böröczky and G. Fejes Tóth editors, Colloq. Math. Soc. Janos Bolyai. vol. 63, pp. 217-244. North-Holland, Amsterdam, 1994.

[9] Sascha Kurz, *Counting polyominoes with minimum perimeter*, Ars Combinatoria Vol. 88 (2008), pp. 161-174.

[10] N. J. A. Sloane, *The On-Line Encyclopedia of Integer Sequences*, http://www.research.att.com/ njas/sequences.

[11] Eric W. Weisstein, *Polyiamond*, MathWorld–A Wolfram Web Resource, `http://mathworld.wolfram.com/Polyiamond.html`.

[12] Jonathan Yackel and Robert R. Meyer, *Optimal Tilings for Parallel Database Design*, Advances in Optimization and Parallel Computing, pages 293–309. North - Holland, 1992.

[13] J. Yackel, *Minimal Perimeter Tiling in Parallel Computation*, PhD thesis, U. of Wisconsin, 1993.

[14] Jonathan Yackel, Robert R. Meyer, Ioannis Christou, *Minimum-Perimeter Domain Assignment*, Mathematical Programming, vol. 78, issue 2, pp. 283–303, 1997.

[15] Winston C. Yang, *Optimal Polyform Domain Decomposition*, PhD thesis, University of Wisconsin-Madison, 2003.

[16] Winston C. Yang and Robert R. Meyer, *Maximal and minimal polyiamonds*, Optimization Technical Report 02-03, May 2002.

[17] Winston C. Yang and Robert R. Meyer, *Maximum area converses to Harary-Harborth polyform theorems*, Journal of Combinatorics, Information, and System Sciences, vol. 32, pp. 63-91, 2007.